

Full Length Research Paper

Silencing of the rift valley fever virus s-genome segment transcripts using RNA interference in *Sf21* insect cells

Juliette Rose Ongus*, Evans Kiplangat Rono and Fred Alexander Wafula Wamunyokoli

Jomo Kenyatta University of Agriculture and Technology, P. O. Box 62000-00200 Nairobi, Kenya.

Received 23 January, 2017; Accepted 10 April, 2017

Rift Valley fever (RVF) is a mosquito-borne disease that affects humans and livestock. It results in economically disastrous livestock deaths in Africa. The causative agent is RVF virus (RVFV), which possesses a tripartite negative-sense, single-stranded RNA genome, with large (L), medium (M) and small (S) segments. The lack of effective vaccines and anti-RVFV therapies motivates concerted efforts in search for safe and effective remedies. Recent advances in the RNA interference (RNAi) may provide promising tools to control RVFV. This study aimed to use the Baculovirus Expression Vector System to demonstrate that the RVFV S-genome segment is susceptible to RNAi. A multiplex short hairpin RNA (shRNA) transcription cassette was constructed for generating small interfering RNA (siRNA) that target both the RVFV genomic RNA transcripts and the Green Fluorescent Protein (GFP) which was used as a reporter gene. Two expression vectors were constructed; one for expressing the RVFV S-genome alone and the other one for simultaneous expression of both the RVFV S-genome and the shRNA cassette. A separate transiently expressed GFP only vector was included as an internal positive control to be expressed simultaneously when co-transfected into *Sf21* insect cells with each RVFV-S construct to monitor the effectiveness of the shRNA to trigger RNAi. By design, the RNAi effect on both the RVFV-S and the GFP transcripts was driven from the same shRNA. A statistically significant reduction in the relative GFP fluorescence ($P < 0.05$) was demonstrated and a drop in GFP and the RVFV S transcript levels observed. Collectively, these results suggest the potential application of RNAi as an antiviral strategy against RVFV.

Key words: Baculovirus Expression, rift valley fever, RNA interference, green fluorescent protein.

INTRODUCTION

Rift Valley fever virus (RVFV) (genus: *Phlebovirus*, family: Bunyaviridae) is an enveloped virus (Muller et al., 1994; Giorgi, 1996; Ellis et al., 1988; Nichol et al., 2005;

Sindato et al., 2015). The primary vectors of the virus are transovarially-infected floodwater mosquitoes of the *Aedes* species (Linthicum et al., 1999; Nichol et al., 2005;

*Corresponding author. E-mail: julietteongus@jkuat.ac.ke. Tel: +254 722 339682.

Sang et al., 2017). The virus causes an arthropod-borne RVF disease, which is a major public health threat due to its serious epizootics and epidemics in sub-Saharan Africa (WHO, 2007; Breiman et al., 2008; Boshra et al., 2011). The epizootics result in devastating abortions in pregnant animals (Swanepoel and Coetzer, 2004) and up to 100% mortality rates in domestic animals (Easterday et al., 1962; Meegan et al., 1979; Meegan et al., 1981).

In Kenya, the virus was first isolated in 1930 along Lake Naivasha in the greater Rift Valley, during which sweeping deaths and abortion storms among sheep were reported (Daubney et al., 1931). The 2006/2007 RVFV outbreak in eastern Africa (Sindato et al., 2015) caused 45% human case fatality, and 100 and 60% mortality rates in young and adult livestock respectively (WHO, 2007; CDC, 2007). Effective vaccines for animals and prevention methods for humans are lacking. The currently ineffective or short-acting vaccines for animals against the RVFV and lack of prevention and treatment methods for humans mean that the affected populations remain susceptible (Ikegami and Makino, 2009; Pepin et al., 2010; Boshra et al., 2011). Thus, concerted efforts in search for safe antiviral therapies that will offer effective treatment and prevention strategies are needed. Research on recombinant subunit vaccine development based on the RVFV surface glycoproteins is currently underway (Faburay et al., 2016).

The RVFV possesses a tripartite genome, which is composed of three negative-sense, and single-stranded RNA segments designated as large (L), medium (M) and small (S) where the L and M are of negative polarity while S is of ambisense polarity (Elliott, 1990; Muller et al., 1994; Giorgi, 1996). The L segment (6,404 nucleotides, nt) codes for a 237-kDa L protein, which is the viral RNA-dependent RNA polymerase in a single ORF (Muller et al., 1994). The M segment (3885 nt) codes for a polyprotein precursor to the glycoproteins encoded in a single ORF (Collett et al., 1985). The S segment (1690 nt) codes for two proteins, the 27 kDa nucleoprotein N and a 31-kDa non-structural protein called NSs by utilizing an ambisense strategy (Giorgi et al., 1991).

RNA interference (RNAi) is a highly sequence specific RNA-dependent gene regulatory mechanism by which double-stranded RNA (dsRNA) targets complementary mRNA for degradation (Hannon, 2002; Agrawal et al., 2003; Kang et al., 2008). RNA interference is one of the most promising platform for the development of therapeutics against viral pathogens (Faburay et al., 2016). RNAi can be triggered experimentally by exogenous introduction of dsRNA or using DNA-based vectors, which express short hairpin RNA (shRNA) in the cytoplasm that are processed by Dicer into siRNAs (Swamy et al., 2016; McGinnis, 2010). Expression of short hairpin RNA (shRNA) from plasmids triggers the RNAi pathway, and this gives the promise of developing new RNAi-based gene therapies for controlling of some pathogens (McCaffrey et al., 2002). This gene-specific

therapeutic tool may escape some of the limitations of conventional medicinal chemistry (Hannon and Rossi, 2004). RNAi has been widely demonstrated *in vitro* against many viruses (Ge et al., 2004; Nishitsuji et al., 2006; Carmona et al., 2006; Shi et al., 2010). The RVFV genome sequence is highly conserved at 95% (Liu et al., 2003; Nderitu et al., 2011) making it a good candidate silencing using the RNA approach.

The Baculovirus Expression Vector System (BEVS) (Invitrogen, Carlsbad, CA, USA) uses a recombinant *Autographa californica* Multiple Nuclear Polyhedrosis Virus (AcMNPV) to express high levels of heterologous gene products in lepidopterans *Spodoptera frugiperda* and *Trichoplusia ni* as host insects. The AcMNPV can accommodate foreign genes of interest that are transferred from the expression cassette to the baculovirus genome by site-specific homologous recombination *in vivo* (Vlak and Keus, 1990). It allows expression in a variety of lepidopteran cells including those derived from *S. frugiperda* such as Sf21 cells (Theilmann and Stewart, 1992). The pFastBac™ Dual vector is an example of the expression vectors that are used in the BEVS, which has two strong baculovirus promoters, P_{PH} and P_{P10} to allow simultaneous high-level expression in insect cells (Harris and Polayes, 1997; O'Reilly et al., 1992) and two large multiple cloning sites to facilitate cloning. Another example is the *OpIE2* immediate-early promoter from the baculovirus *Orgyia pseudotsugata* Multicapsid Nuclear Polyhedrosis Virus (*OpMNPV*) in the pIZ/V5-His vector, is employed to express genes of interest (Invitrogen). The *OpIE2* promoter synthesizes high levels of constitutive expression at levels equivalent to those obtained from the P_{PH} and P_{P10} promoters (Theilmann and Stewart, 1992).

The goal of this study was to demonstrate the susceptibility of the RVFV S-genome segment to RNAi in a BEVS model system. The P_{P10} and P_{PH} dual promoter feature of the pFastBac™ Dual vector was used to show the activity of short hairpin RNA (shRNA) transcription cassette against the RVFV S-genome transcript in a dual gene knock-down approach in insect cells.

MATERIALS AND METHODS

The RVFV isolate

A collaborative effort of the Centers for Disease Control and Prevention (CDC) in Kenya and the Kenya Medical Research Institute (KEMRI) isolated the RVFV isolate that was used in this study from infected human serum that was obtained in a separate outbreak investigation from Garissa County in the North Eastern part of Kenya during the 2006/2007 epidemics (Nderitu et al., 2011). This isolate was named the Garissa 004. The isolate was already classified, sequenced, cultured and archived at -80°C as KEN/ Gar-004/06 (GenBank accession no. HM586975 for S segment, HM586964 for M segment, HM586953 for L segment) (Nderitu et al., 2011). For this study, the archived RVFV isolate was amplified by passaging in Vero cells in the Biosafety level-3 (BSL-3) laboratory facility at CDC/KEMRI in Nairobi, Kenya.

Table 1. Primers to amplify full-length RVFV S-genome segment cDNA and GFP.

Name	5'-3' sequence	Restriction site
RVFV-S-F	CTCGAGTACACAAAGCTCCCTAGAGATAC	<i>XhoI</i>
RVFV-S-R	GGTACCTACACAAAGACCCCCTAGTGC	<i>KpnI</i>
GFP-F	GAATTCATGGCTAGCAAAGGAGAAGAAC	<i>EcoRI</i>
GFP-R	GAATTCATGCATTTATTTGTAGAGCTCATCCATGCC	<i>EcoRI-NsI</i>

Total RVFV genomic RNA isolation

The positive cell culture supernatant was used to isolate RVFV genomic RNA using QIAamp® Viral RNA Kit (Qiagen) as per the manufacturer's instructions. The quality of the isolated RVFV genomic RNA assessed by quantification in BioSpec-Mini Spectrophotometer (Shimadzu Corporation) at 120 ng/μl and observed by gel electrophoresis. The RNA was finally aliquoted and stored at -80°C to await the RT-PCR application.

Promoters and recombinant transcription vectors

Very-late strong baculovirus promoters P_{PH} and P_{P10} in the pFastBac™ Dual vector (Invitrogen, Carlsbad, CA, USA) were utilized to express both the RVFV S-genome and the shRNA cassette. These allow simultaneous high-level expression in insect cells and two large multiple cloning sites to facilitate cloning were used (Harris and Polayes, 1997; O'Reilly et al., 1992). A second expression vector the pIZ/V5-His vector plasmid (Invitrogen, Carlsbad, CA, USA) was used to express the GFP reporter gene using the *OpIE2* immediate-early promoter. The *OpIE2*, promoter utilizes the host cell transcription machinery and does not require viral factors for activation but is activated upon arrival in the cytoplasm of the host cell (Friesen and Muller, 2001). It allows expression in a variety of lepidopteran cells including those derived from *S. frugiperda* (such as Sf21 cells) (Theilmann and Stewart, 1992).

Construction of recombinant pFastBacDual-S (pFBD-S) transcription vector

To amplify the entire length of the RVFV S-genome segment for cloning into the pFastBac Dual™ expression vector, 2 μg of the RVFV total genomic RNA sample was used in the RT-PCR in complementary DNA (cDNA) synthesis with SuperScript III/Platinum Taq DNA polymerase high fidelity enzyme mix as per the manufacturer's instructions (Invitrogen, Carlsbad, CA, USA).

Primers RVFV-S-F and RVFV-S-R were used for the amplification and to introduce *KpnI* and *XhoI* restriction enzymes restriction sites respectively for cloning (Table 1). The other two RVFV full-length genome segments (L and M) were unsuccessfully cloned, and therefore are not analysed in this study. The RT-PCR cycling parameters were 1 cycle of 51°C for 60 min and 94°C for 2 min, followed by 40 cycles of 94°C for 15 s, 56°C for 30 s, and 68°C for 2 min, followed by a final extension at 68°C for 5 min. The PCR products were detected by electrophoresis in a 1% agarose gel stained with ethidium bromide and running at 10 volts/cm for 45 min. The amplicons were purified from the agarose gel using the S.N.A.P™ gel purification kit (Invitrogen, Carlsbad, CA, USA) according to the manufacturer's instructions.

The purified PCR products of the RVFV S-genome segment were ligated into the pGEM®-T Easy Vector (Promega) for TA cloning as per the manufacturer's instructions to generate pGEM®-T Easy-S construct (Abbreviated as pGEMT-S). Following the blue-white

screening, white colonies carrying the cloned inserts were selected from the LB agar plates (containing 100 μg/ml ampicillin and 20 μg/ml X-gal) for colony PCR screening and sequencing to further confirm the positive clones.

Recombinant plasmids were purified using the GenScript kit (GenScript Corporation, Piscataway, NJ) from the overnight LB broth culture containing 100 μg/ml ampicillin. The RVFV S-segment cDNA insert was directionally subcloned from the pGEMT-S plasmid into the pFastBac Dual™ vector under the control of the P_{P10} promoter in order to generate a recombinant plasmid pFastBac Dual™-S (abbreviated as pFBD-S) construct.

To do this, the plasmid pGEMT-S was digested with *KpnI* and *XhoI* restriction enzymes and subcloned into the pFastBac Dual™ vector digested with the same enzymes (Table 1) according to the manufacturer's instructions. The recombinant pFBD-S clones were selected on LB agar plates (containing 100 μg/ml ampicillin and 7 μg/ml gentamycin) and confirmed by the *KpnI-XhoI* restriction enzyme double digestions.

Construction of recombinant pFBD-shRNA transcription vector

In order to generate fragments for the short hairpin RNA (shRNA) transcription cassette, a 1253 bp multiplex shRNA template containing 150 bp fragments each from the RVFV L, M and S genome segments and 150 bp of GFP (Figure 1, Figure S3) was designed and amplified by PCR (Table 2). These fragments were selected from the regions with 30 to 50% GC content (for optimal activity), which were identified using the Ambion siRNA Target Finder (www.ambion.com/techlib/misc/siRNA_finder.html). The RVFV L (genome location 6056-6205), M (genome location 3437-3586) and S (genome location 1127-1276) segment portions were amplified by the RT-PCR from the RVFV RNA templates (Nderitu et al., 2011). The GFP fragment was amplified by PCR using the pcDNA-DEST47 Gateway® Vector as DNA template (Invitrogen, Carlsbad, CA, USA) (plasmid location 2628-3347) (GFP ORF location 193-342) was amplified by PCR. The optimized shRNA PCR primer annealing temperatures were as follows: For shGFP-F/shGFP-R, RVFV-shL-F/RVFV-shL-R, RVFV-shM-F/RVFV-shM-R and RVFV-shS-F/RVFV-shS-F were 58, 52, 56 and 60°C respectively. The extension and final extension times in all their PCR cycling parameters were 45 s and 3 min respectively. All the PCR products were detected and purified as described earlier.

The four fragments were first sequentially cloned into the pGEMT vector to generate the recombinant plasmid pGEM®-T-shRNA (abbreviated as pGEMT-shRNA). In brief, the shRNA chimeric gene construct (Figure 1) was cloned in the following sequential order: First the 640 bp forward-facing, that is, genomic sense (GS) construct was cloned starting with the 150 bp L segment which was cloned using the restriction enzymes *BamHI* and *SpeI*; 150 bp M using *SpeI* and *NotI*; 150 bp S using *NotI* and *PstI*; and 150 bp GFP using *PstI* and *HindIII*. A 13-nucleotide loop spacer containing an *EcoRI* restriction site was introduced using the shGFP-R primer to create a separator between the GS and reverse complement (RC) regions to allow for the shRNA transcript to fold on itself to create a dsRNA that would trigger RNAi in the cells (Figure 1). Next, the 632

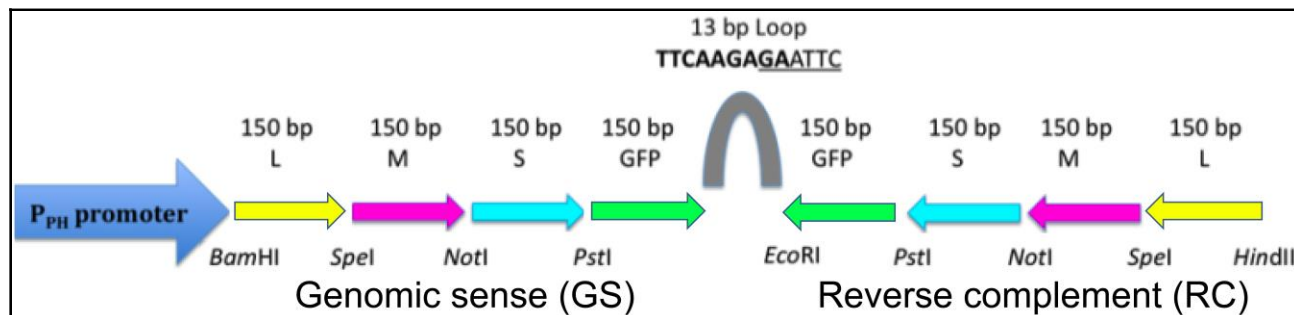


Figure 1. Schematic representation of the complete 1253 bp multiplex shRNA transcription constructs. The colour codes correspond to the same fragments and the arrow points to the direction of the ORF of the cloned insert/fragment in the schematic illustration. The restriction sites that are indicated were used for sequential cloning of the fragments. The 150 bp L, M and S fragments respectively were cloned from the cDNA from the RVFV KEN/ Gar-004/06 isolate (GenBank accession no. HM586953 for L segment, HM586964 for M segment and HM586975 for S segment) using the primers indicated in Table 2. The 150 bp DNA fragments of the GFP was amplified from the GFP ORF in the pcDNA-DEST47 Gateway® Vector. The whole piece of the GS region was used as a DNA template in PCR to amplify and directionally cloned the RC region separated by a 13 bp loop as showed. Upon transcription in the insect cells, the RNA transcript that is transcribed forms a shRNA cassette with a hairpin structure, because the GS portion is complementary to the RC portion. When the *RNAi* is induced, the shRNA cassette is processed by dicing to produce a mixed population of *siRNAs* for different fragments (L, M, S and GFP). In this study, the ability of the S and the GFP *siRNAs* to degrade the transcripts of the RVFV S-genome segment and the GFP respectively were assessed.

Table 2. Primers for construction of 150 bp fragments of multiplex shRNA transcription cassette.

Name	5'-3' sequence	Restriction site
RVFV-shL-F	CGC GGATCC AGAGAACCTTTGATAAATCATAGTC	<i>Bam</i> HI
RVFV-shL-R	CGC ACTAGT AGGACATCAGTTCATTATCTATGATTGC	<i>Spe</i> I
RVFV-shM-F	CGC ACTAGT CACATTTTAGAGAGGCCTGTTCTTCC	<i>Spe</i> I
RVFV-shM-R	CGC GCGGCCGC TTGGAATTTCTTTGACTGGTTTTCTGG	<i>Not</i> I
RVFV-shS-F	CGC GCGGCCGC CTTCTTCTGCTACTGGGACAACCATGG	<i>Not</i> I
RVFV-shS-R	CGC CTGCAG CAGATACAGAGAGTGAGC	<i>Pst</i> I
shGFP-F	CGC CTGCAG TTCTCTTATGGTGTTCATGCTTTTCC	<i>Pst</i> I
shGFP-R	CGC AAGCTTCGGAATTC TCTTGAACCTTGACTTCAGCACGCGTCTTGTAG	<i>Hind</i> III- <i>Eco</i> RI
shRC-F	GCG GAATTC TCTTGAACCTTGATTCC	<i>Eco</i> RI
shRC-R	CGC AAGCTT AGAGAACCTTTGATAAATCATAGTC	<i>Hind</i> III

bp reverse-facing, that is, RC construct (complementary to the GS construct) was amplified by PCR from the entire GS portion using the RC primer pair shRC-F and shRC-R (Table 2) and Platinum *Taq* DNA polymerase (Invitrogen, Carlsbad, CA, USA). The following optimized PCR cycling parameters were used; 1 cycle of 94°C for 2 min, followed by 40 cycles of 94°C for 30 s, 60°C for 30 s and 72°C for 1 min, and a cycle of final extension at 72°C for 5 min. The PCR products were analyzed as mentioned before, and directionally cloned into the pGEMT-GS recombinant plasmid construct using *Hind*III and *Eco*RI restriction enzymes in order to form a complete shRNA transcription construct that constitutes the GS and the RC parts.

Using the same restriction enzymes, the shRNA insert was then directionally subcloned from the pGEMT-shRNA construct into the pFastBac Dual™ vector under the control of the *P_H* promoter to generate the recombinant plasmid pFastBac Dual™ -shRNA (abbreviated as pFBD-shRNA). Colonies carrying the recombinant pFBD-shRNA clones were selected on LB agar plates as described previously.

Construction of recombinant pFBD-S/shRNA transcription vector

To generate the recombinant plasmid with the ability to transcribe both the RVFV-S genome transcript and the shRNA, *pFastBacDual-S/shRNA* (abbreviated as pFBD-S/shRNA), the RVFV S-segment was then directionally subcloned from pGEMT-S recombinant construct into pFBD-shRNA under the control of the *P_{P10}* promoter using the *Kpn*I and *Xho*I restriction enzymes. Colonies carrying the recombinant pFBD-S/shRNA plasmid clones were screened, propagated and purified as mentioned previously.

Construction of recombinant pIZ/V5-GFP transcription vector

The GFP expression vector for transcribing the GFP as an internal positive control in insect cells, was constructed. To do this, an Open Reading Frame of 720 bp GFP was amplified from the pcDNA-DEST47 Gateway® Vector (Invitrogen, Carlsbad, CA, USA) using

Table 3. Duplicate *in vitro* transcription experimental setup on 6-well cell culture plates.

Well no. 1	Well no. 2	Well no. 3
Well no. 4	Well no. 5	Well no. 6
Well 1 and 4: Mock-transfected control cells.		
Well 2 and 5: siRNA-negative control cells (Co-transfection of AcMNPV Bacmid-S and pIZ/V5-GFP).		
Well 3 and 6: siRNA-positive test cells (Co-transfection of AcMNPV Bacmid-S/shRNA and pIZ/V5-GFP)		

the Platinum *Taq* DNA polymerase enzyme (Invitrogen, Carlsbad, CA, USA).

The pcDNA-DEST47 Gateway[®] Vector (1 µg) was used as the GFP template in 50 µl PCR reaction volume. The cycling parameters were 1 cycle of 94°C for 2 min, followed by 40 cycles of 94°C for 30 s, 60°C for 30 s, and 72°C for 1 min, followed by a final extension at 72°C for 7 min utilizing the GFP PCR primers GFP-F and GFP-R (Table 1).

The PCR products were analyzed and purified as described earlier, then cloned into the pGEM[®]-T Easy Vector in order to construct a pGEMT-GFP recombinant plasmid. The PCR primers introduced into the PCR product 18 bp additional *EcoRI* and *EcoRI-NsiI* restriction sites for cloning. Using the *EcoRI* restriction enzyme, the GFP insert was then sub-cloned from the pGEMT-GFP construct into the pIZ/V5-His vector (Invitrogen, Carlsbad, CA, USA) under the *OpIE2* promoter in order to construct GFP expression vector (pIZ/V5-GFP) for transfecting into insect cells. Colonies carrying the recombinant pIZ/V5-GFP clones were selected on 50 µg/ml Zeocine selective LB agar plates.

Sequencing the recombinant plasmid constructs

All the purified plasmid constructs were sequenced by Sanger sequencing at MacroGen, Inc. (South Korea). The sequences were edited using Bioedit software version 5.0.6 (Ibis Biosciences) and a similarity nucleotide search was obtained by BLAST in the National Center for Biotechnology Information (NCBI) website (<http://blast.ncbi.nlm.nih.gov/Blast.cgi>). ClustalX and Mega 4 (Tamura et al., 2007) software were also used to align the sequences. These analyses confirmed that there were no PCR-generated mutations, which would interfere with the sequence specificity of the RNAi mechanism.

Propagation of recombinant pFBD-S and the pFBD-S/shRNA bacmids in DH10Bac[™] *E. coli* cells

To generate recombinant AcMNPV Bacmid DNA for transfecting into insect cells, 2 ng of each of the pFBD-S and the pFBD-S/shRNA expression vectors were propagated and isolated independently from chemo-competent DH10Bac[™] cells following manufacturer's instructions (http://tools.invitrogen.com/content/sfs/manuals/bactobac_man.pdf) (Invitrogen, Carlsbad, CA, USA). In summary, the pFBD-S was used to generate large molecular weight AcMNPV recombinant baculovirus genome containing the S-genome segment (AcMNPV Bacmid-S DNA). While the pFBD-S/shRNA was used to generate large molecular weight AcMNPV recombinant baculovirus genome containing the S segment and the multiplex chimeric shRNA transcription cassette (AcMNPV Bacmid-S/shRNA DNA).

Transfection of recombinant pFBD-S and the pFBD-S/shRNA Bacmid DNAs into Sf21 cells for *in vitro* transcription

To transcribe in insect cells the S-genome, the shRNA transcription

cassette, and the GFP, the recombinant AcMNPV Bacmid-S and Bacmid-S/shRNA were standardized and transfected into Sf21 cells according to the supplier's Bac-to-Bac[®] guidelines (Invitrogen, Carlsbad, CA, USA). The Sf21 cells (2.0×10^6) of greater than 95% viability for use in the transfections were seeded in a 6-well plate (Invitrogen, Carlsbad, CA, USA). A master mix was separately prepared by diluting gently 10 µl of 16.9 µg/ml recombinant pFBD-S Bacmid DNA and 10 µl of 12.6 µg/ml pIZ/V5-GFP plasmid construct in 100 µl of 0.2 µm filter sterilized Grace's Unsupplemented Medium, without antibiotics or serum per well. The same procedure was repeated for co-transfection of the Sf21 cells with 24.5 µl of 6.9 µg/ml recombinant pFBD-S/shRNA Bacmid DNA and 10 µl of 12.6 µg/ml pIZ/V5-GFP plasmid construct. The quantitation of the Bacmid DNA and the pIZ/V5-GFP plasmid constructs was done to ensure that the concentrations across all the wells were standardized.

The Cellfectin[®] reagent (Invitrogen) (liposome for mediating the transfection) and DNA mixtures were gently combined and incubated for 20 min at room temperature. The DNA-lipid transfection mixtures were added drop wise onto the cells in the wells and incubated at 27°C for 5 h.

The transfection mixtures were removed and replaced with 2 ml of 0.2 µm filter sterilized complete Grace's Insect Medium (Supplemented medium with 10% FBS and penicillin/Streptomycin antibiotics to final concentration of 100 Unit/ml and 100 µg/ml respectively). The cells were incubated at 27°C as per the time-course set up in duplicate using five 6-well plates incubated at 27°C for 0, 24, 48, 72 and 96 h respectively.

Duplicate sets of wells were set up as follows: The cells in the first pair of wells were not transfected (mock transfected negative control with no constructs). The cells in the second pair of wells were co-transfected with the pFBD-S and pIZ/V5-GFP plasmid constructs (RNAi-negative). The cells in the third pair of wells were co-transfected with pFBD-S/shRNA and pIZ/V5-GFP plasmid constructs (RNAi-positive). Table 3 summarizes the outline of the 6-well plate transfection set up. A time-course experiment at 0, 24, 48, 72 and 96 h incubations respectively was set up by preparing five (5) identical plates as per the setup in Table 3. Each time point was analysed in duplicate. For the 0 h duplicated sets, all the cells from the mock-transfected wells as well as from the recombinant vector wells were harvested immediately upon transfecting, while the other sets were harvested after the stated time of incubations. After each incubation time, the medium was harvested by sloughing off the cells to the medium and clarifying them at 500 X g for 5 min. The cells were resuspended immediately in 1 ml freezing medium constituting 20% glycerol, 50% sterile-filtered Grace's medium, unsupplemented (without antibiotics and serum) and 30% FBS. The cells were divided for further analyses into three aliquots; one with 500 µl stocks for -80°C storage, another one with 460 µl for RNA isolation and finally the third one with 40 µl for fluorescence microscopy.

Monitoring of RNAi by GFP fluorescence microscopy

The Sf21 cells were harvested at 24 h intervals (0, 24, 48, 72 and 96 h) post-transfection. An aliquot of 10 µl of Sf21 from each of

Table 4. Relative GFP fluorescence unit from the experimental set-ups.

Set-up	Time of incubation (h) and other parameters	siRNA-negative	siRNA-positive	Change	Absolute deviation from median
Set 1	24	796381.84	656335.83	140046.02	148732.25
	48	1042817.80	834261.32	208556.50	208556.50
	72	1280084.70	911084.66	369000.04	228954.02
	96	1807415.60	1095757.00	711658.57	503102.07
	Total	4926699.94	3497438.81	1429261.12	1089344.84
	Mean	1231675.00	874359.70	357315.28	272336.21
	Variance	1.86E+11	3.32E+10	6.50E+10	2.48E+10
	SD	431651.06	182124.29	254970.85	157565.53
	Median			288778.27	
	n	4	4	4	4
Set 2	24	740429.58	689822.41	50607.17	235743.90
	48	1031367.30	793270.40	238096.90	238097.00
	72	1327613.10	993007.90	334605.20	283998.00
	96	1799000.00	1079644.90	719355.10	481258.00
	Total	4898410.00	3555745.61	1342664.37	1239096.90
	Mean	1224603.00	888936.40	335666.09	309774.23
	Variance	2.04E+11	3.20E+10	7.90E+10	1.36E+10
	SD	451776.84	178884.48	281659.79	116460.60
	Median			286351.07	1239096.90
	n	4	4	4	4

time-course experiment was put on a microscope slide. The cells were allowed to attach for 45 min and then fixed for 15 min by adding an equal volume of 4% paraformaldehyde in PBS pH 7.4. The cover slips were laid on the slides and excess flow-over medium was wiped out carefully. The attached Sf21 cells were analyzed by fluorescence microscopy using iMIC microscope (TILL photonics) with Pike F-145b camera (Allied Vision Technologies, GmbH, Germany). The GFP filter was chosen at excitation wavelength of 500 nm. The exposure time was also finally adjusted to 50 milli-seconds. Following image acquisition, the raw data were exported to ImageJ 1.45 software (National Institutes of Health) (Collins, 2007). Using the software, images were edited and time-course average GFP fluorescence per cell was measured. These readings were used to compute the relative GFP fluorescence according to the formula by the ImageJ 1.45 software (Table 4). Strengths of correlation were measured between the effects of RNAi treatment and the time to describe the variations due to the effects of RNAi treatment in time. The *t*-test statistical analysis was used to measure the average relative GFP fluorescence per cell at 95% confidence level with $P < 0.05$ level of significance. Duplex RT-PCR assays were done on total RNAs that were isolated from the cell samples. RVFV-S specific primers (RVFV-S-F and RVFV-shS-R) and GFP-specific primers GFP-F (Table 1) and shGFP-R (Table 2) were used.

Monitoring of RNAi by GFP and RVFV S semi-quantitative duplex RT-PCR

Total RNA was isolated from the harvested Sf21 cells using Trizol™ reagent method (Invitrogen, Carlsbad, CA, USA). Duplex semi-quantitative RT-PCR assays for analyzing GFP and RVFV S-genome RNA transcript levels were done on equal volumes (1 µl) of the total RNA from the time-course experiments merging different

time points post-transfection. The RT-PCR was carried out using SuperScript III/ Platinum Taq DNA polymerase high fidelity enzyme mix (Invitrogen, Carlsbad, CA, USA). The GFP-specific (GFP-F and shGFP-R) and RVFV-S specific (RVFV-S-F (Table 1) and RVFV-shS-R (Table 2) primer combinations were utilized. The RVFV S primer combinations detected the S RNA transcript by amplifying a 572 bp cDNA fragment while that of the GFP primers detected the GFP RNA transcript by amplifying a 370 bp cDNA fragment. The optimized RT-PCR cycling parameters were 1 cycle of 51°C for 60 min and 94°C for 2 min, followed by 20 cycles of 94°C for 15 s, 56°C for 30 s, and 68°C for 1 min, followed by a final extension at 68°C for 3 min. The expected band sizes of the RT-PCR products were checked by running on a 1% agarose gel at 10 volts/cm for 1 h. Semi-quantitative RT-PCR was used in place of qPCR since at the time of this experimentation the study could not access qPCR infrastructure. However, it is recommended that future studies should improve similar investigations with qPCR.

Statistical analyses on the time-course experiment

To statistically support the molecular data, the pairwise statistical testing on relative GFP fluorescence per cell was analysed using Pearson's correlation strength and *t*-distribution at a level of significance of $P = 0.05$ with a 95% confidence interval.

RESULTS

Expression of the RVFV S genome, shRNA and GFP cassettes in the BEVS

This study aimed to show the susceptibility of the RVFV

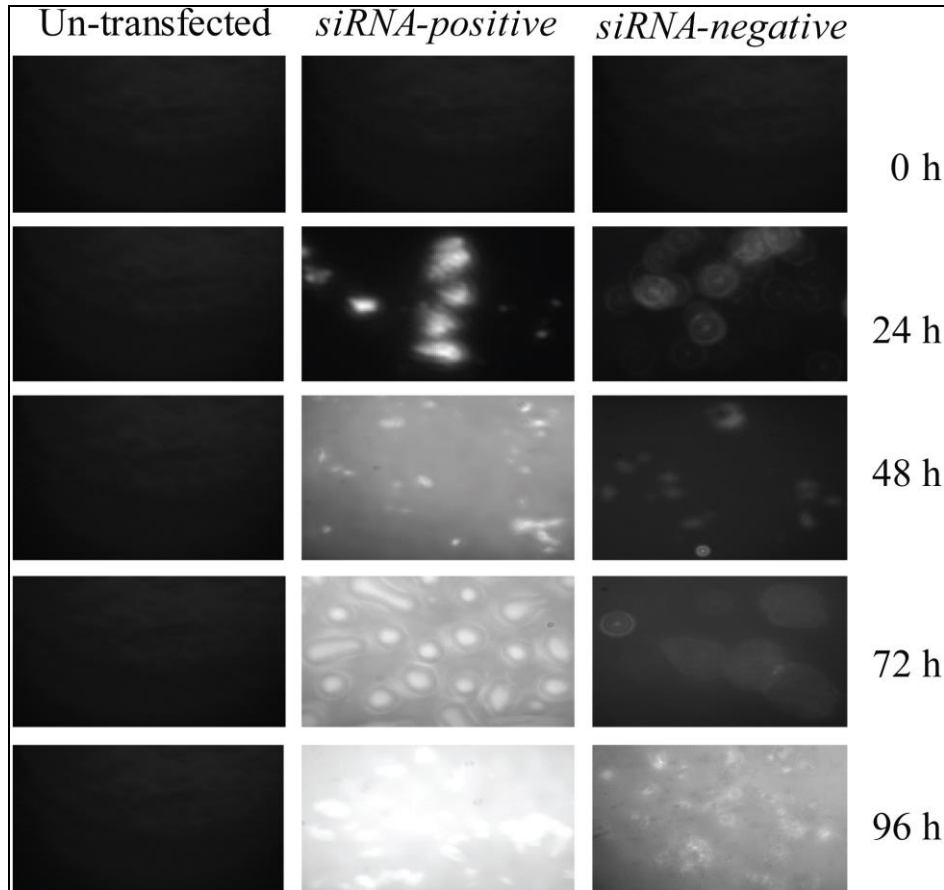


Figure 2. Time-course assessment of the effects of the *RNAi* on the relative GFP fluorescence per cell. First column: Un-transfected *Sf21* control cells, where no recombinant construct was transfected. . Second column: GFP fluorescence in the *Sf21* test cells that were co-transfected with pIZ/V5-GFP and recombinant AcMNPV Bacmid-S (*siRNA-negative*). Third column: Declined GFP fluorescent intensities detected from the *Sf21* test cells that were co-transfected with pIZ/V5-GFP plasmid construct and recombinant AcMNPV Bacmid-S/shRNA (*siRNA-positive*). The apparently higher amounts of the GFP fluorescence intensities in the *siRNA-negative* than those for the *siRNA-positive* were observed per time point. Moreover, the increase in the GFP fluorescence intensities positively correlated with the increase in the time of incubation. This amount of change was quantified and presented in Figure 4 and Tables 4 and 5.

S-genome segment to RNAi using the Baculovirus Expression Vector System as a model (Ciccarone et al., 1997) guided by the GFP reporter gene as an internal control.

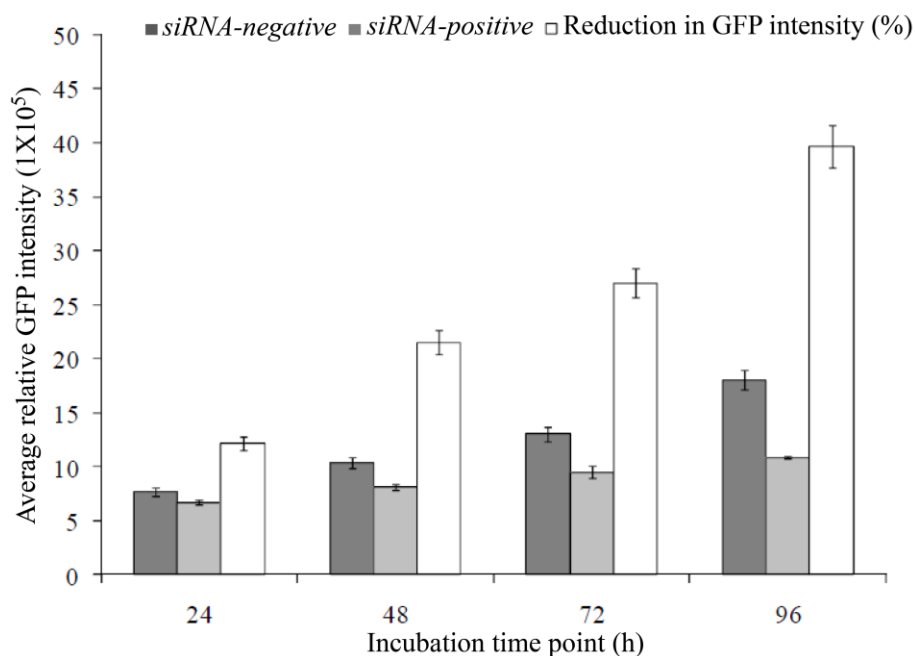
Monitoring RNAi by GFP fluorescence microscopy in *Sf21* cells

GFP fluorescence microscopy in *Sf21* cells was monitored from the samples harvested at 0, 24, 48, 72 and 96 h post-transfection respectively. At each time point, the duplicated wells of each of the mock-transfected (control group), the *siRNA-negative* control cells (Co-transfection of AcMNPV Bacmid-S and pIZ/V5-

GFP) and the *siRNA-positive* test cells (Co-transfection of AcMNPV Bacmid-S/shRNA and pIZ/V5-GFP) were included (Table 3). GFP fluorescent signals were not detected from the mock-transfected controls and at time 0 h (Figures 2 and S1). Progressive decline in the GFP expression was however observed by a decreasing GFP fluorescence intensity (iMIC, Till Photonics GmbH) in the course of time. The difference of means between duplicate experiments for the average relative GFP fluorescence per cell in the *siRNA-positive* and the *siRNA-negative* wells upon correction by GFP background subtraction was computed (Figures 2 and S1, and Tables 4, 5 and S2). The average (Figures 2 and S1). Percentage reduction in GFP intensity due to RNAi increased with time (Figure 3). Average percentage

Table 5. Average relative GFP fluorescence unit of *Sf21* cells from the two sets.

Time after transfection (h)	Average GFP relative fluorescence		Reduction in GFP intensity (%)
	<i>siRNA-negative</i>	<i>siRNA-positive</i>	
0	0.00	0.00	0.0
24	768405.71	673079.12	12.4
48	1037092.56	813765.86	21.5
72	1303848.91	952046.28	27.0
96	1803207.78	1087700.97	39.7
Total	4912554.96	3526592.23	28.2
Average	9825110.00	705318.45	28.2

**Figure 3.** Average relative GFP expression over time in *siRNA*-positive and *SiRNA*-negative *Sf21* cells. Percentage amount of reduction (the difference between the GFP fluorescence of the *siRNA-negative* and the *siRNA-positive*) in the GFP fluorescence intensity due to RNA silencing was observed to increase with the time of incubation. In average, the percentage reduction in the relative GFP fluorescence of up to 39.7% was observed by the 96th h (Table 5).

reduction of the relative GFP fluorescence of up to 39.7% was achieved by the 96th hour. A graph of percentage reduction in the amount of the GFP fluorescence against incubation time showed that the reduction in the GFP intensity increased with time.

All the promoters (P_{PH} , P_{10} and $OpIE2$) are very strong and remained active throughout the course of the experiment; therefore, it was not possible to achieved absolute transcript knockdowns. The experimental setup was designed in such a way that *siRNAs* which are both anti-RVSV S-genome segment and anti-GFP transcripts would be generated from the same multiplexed shRNA transcription cassette. As such, the expression of these

siRNAs for targeting the RVSV S-genome segment was positively correlated with the expression anti-GFP *siRNAs* (Figure S2 and Tables S3 and S4). The transcription of RVSV S-genome and shRNA cassette respectively occurred simultaneously in one pFBD-S/shRNA vector. The two baculovirus promoters being equally powerful and are turned on at the same time enabled the *RNAi* pathway to occur as their respective *siRNA* were processed.

To statistically evaluate the null hypothesis that the *siRNA*-positive treatment had “no effect” on the RVSV S-genome segment transcript, the Pearson product-moment correlation coefficient (Tables S3 and Table S4)

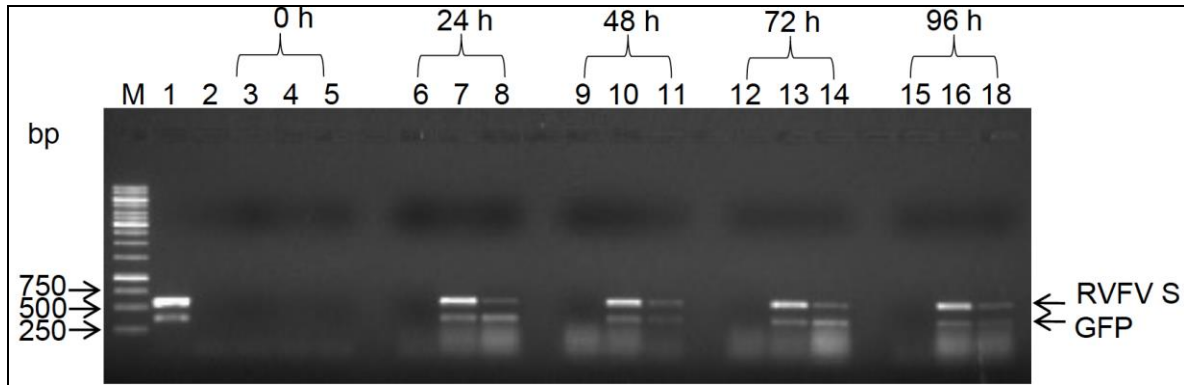


Figure 4. Duplex semi-quantitative RT-PCR to measure the *in vitro* RNAi effects on RVFV S-genome segment RNA transcript. M: 1 Kb DNA ladder (Fermentas). Lanes 1 and 2: Positive and no-template negative controls respectively. Lane 3 through lane 18: Duplex semi-quantitative RT-PCR results from the time-course experiment at 0, 24, 48, 72 and 96 h arranged in groups of threes indicating the 370 bp GFP and the 572 bp RVFV S. In each of these groups; first well shows the results of RNA from the un-transfected S21 negative control cells, second well shows the RT-PCR results of total RNA from S21 cells that were co-transfected with pIZ/V5-GFP construct and recombinant AcMNPV Bacmid-S (*siRNA-negative*), and third well displays the RT-PCR results of RNA from S21 cells co-transfected with pIZ/V5-GFP construct and recombinant AcMNPV Bacmid-S/shRNA (*siRNA-positive*). There is apparent reduction in the cDNA band densities in the *siRNA-positive* groups compared to the *siRNA-negative* groups that were amplified from both the GFP and the RVFV S transcripts.

and *t*-test analyses were done on the data sets (Supplementary information). The Pearson product-moment correlation coefficient, *r* (Pearson's *r*) was used to measure the strength of the linear relationship between incubation times and amount of change in the relative GFP fluorescence intensities (Figure S2). The Pearson's *r* between *X* = Incubation time and *Y* = change in relative GFP fluorescence, *r* = 0.9584 and 0.9511 in sets 1 and 2 respectively showed strong positive relationship (Tables S3 and S4). The mean Pearson product-moment correlation coefficient (*r* = 0.95475) between the siRNA-negative and siRNA-positive groups of cells in the two independent experiments showed a strong positive correlation. Strengths of correlation were measured between the RNAi treatments and the time variables. The percentage reduction in GFP intensity increased with time.

The relative GFP fluorescence per cell from the duplicate experiments were also used to test the null hypothesis at *P* < 0.05 confidence level of significance using the *t*-test statistics (Supplementary material) (Chap, 2003; Fisher and Belle, 2004; Kaps and Lamberson, 2004). The corresponding *t*-test analysis for these correlation strengths showed significant variation between the siRNA-negative and siRNA-positive groups ($t_{1-0.05/1, 4-2} = 2.92$; *P* < 0.05). A second *t*-test analysis done on each independent time-course experiment also showed significant effect of RNAi treatment between the two groups ($t_{1-0.05/1, 3} = 2.80$, *P* < 0.05). There was no significant difference in the amount of change achieved by the two separate independent experiments ($t_{1-0.05/1, 6} = 0.0806$, *P* > 0.05) suggesting that the two independent experiments were similar. The pattern of GFP

transcription post-RNAi was thus assumed to mirror that of the RVFV S-genome segment because the source of siRNA originated from the same shRNA chimeric construct. As there was a statistically significant effect due to the RNAi in the RNAi-positive test group on the transcript levels of the RVFV S-genome transcript, the null hypothesis of "no-effect", that is, $H_0: \mu_1 = \mu_2$ was therefore rejected.

Verification of the effects of the RNAi on the transcripts of GFP and RVFV S by semi-quantitative RT-PCR

In the RNAi-positive groups, transcription of shRNA transcription cassette generated siRNAs that triggered gene-specific degradation of the RVFV S and GFP transcripts via the RNAi pathway. The monitoring of the RNAi was achieved by using duplex semi-quantitative RT-PCR to detect both GFP (as the experimental control) and RVFV S-genome RNA transcript levels (Figure 4 and Table S1). The duplex RT-PCR detections yielded expected fragments of RVFV-S and GFP of 572 and 370 bp, respectively from the transfected cells only at 24, 48, 72 and 96 h time points. The results further indicated that the RVFV-S-genome segment transcript levels in the siRNA-negative S21 cells were apparently higher relative to that of the siRNA-positive S21 cells.

DISCUSSION

RNAi is a naturally occurring pathway thought to have

evolved in plants and animals over millions of years as a form of innate immunity defence against viruses, suggesting an important role in pathogen resistance (Meng et al., 2013). RNAi can be triggered experimentally by exogenous introduction of dsRNA or using DNA-based vectors, which express short hairpin RNA (shRNA) in the cytoplasm that are processed by Dicer into siRNAs (Swamy et al., 2016; McGinnis, 2010). RNAi can also be induced directly by transfecting cells with siRNAs with dinucleotide 3' overhangs (Fitzgerald et al., 2017).

This study described a BEVS-based strategy of demonstrating simultaneous RNA silencing of multiple sequences, in a multiplex RNAi experiment using a single transgenic construct of defined size. The dual promoter capacity of pFBD vector to clone and simultaneously express the two recombinant genes under the P_{10} and the P_{PH} promoter from a single vector offered a major advantage over the use of two separate vectors. It suggests a possible way to enhance multiple gene knockdowns in a single organism, and could also be applied in mammalian cells. RNAi is a specific, potent, and highly successful approach for loss-of-function studies in virtually all eukaryotic organisms (McGinnis, 2010; Pompey et al., 2014; Koch et al., 2016). RNAi technology takes advantage of the cell's natural machinery, facilitated by short interfering RNA molecules, to effectively knock down expression of a gene of interest (Swamy et al., 2016). Simultaneous RNA silencing using a multiplex RNAi construct has been demonstrated by Bucher et al. (2006). The Bucher et al. (2006) demonstrated a simple procedure to obtain broad virus resistance at a high frequency by RNA silencing, using a single transgene construct of limited size. This shown that efficient simultaneous targeting of four different tospoviruses can be achieved by using a single small transgene based on the production of minimal sized chimeric cassettes. The shRNA is processed into specific siRNA, which are directed against a viral genome resulting in down regulation of the genome products (Li and Patel, 2016). In this study, a four-fragment shRNA chimeric construct was made using the BEVS technology for use to target all the three RVFV genome segments (L, M and S) and the GFP as a requirement of the larger study. The multiplex shRNA consisted of successive fragments of 150 bp each of RVFV L, M and S genome fragments and 150 bp GFP (excluding the restriction sites). The 13 bp loop structure separated the genomic sense (GS) constructs and reverse-complement (RC) constructs. Upon transcription in insect cells, the RNA forms a shRNA structure because the RC is complementary sequence to GS. The primers, the multiplex shRNA construct and the respective methods used here are original to this study. However, the idea of the 150 bp shRNA segments was obtained from Bucher et al. (2006) whose cloning method was different from the one used here. The Bucher et al. (2006) PCR merging strategy did not work in this study, therefore the

restriction cloning option was developed. It has been shown that shRNA production increases efficiency of silencing better than dsRNA (Brummelkamp et al., 2002).

The constitutive expression of GFP by the independent pIZ/V5-GFP construct allowed the visualization of the RNAi effects over time since the siRNA targeting both the RVFV S-genome and GFP were generated from the same shRNA transcript. The co-delivery of this pIZ/V5-GFP construct with either Bacmid-S or Bacmid-S/shRNA into the insect cells allowed monitoring of the RNAi using the duplex semi-quantitative RT-PCR and the GFP fluorescence detection methods. GFP is often used as a reporter gene in a range of qualitative and quantitative studies, real time and an indicator for protein production due to its ability to emit luminescence under UV transillumination (Chalfie et al., 1994; Chalfie and Kain, 1998). The P_{PH} and P_{10} promoters are activated during late stages post-infection (transfection) between 18 to 76 h (Braunagel and Summers, 2007; Yang and Miller, 1999). The immediate early *OpIE2* promoter becomes active between 30 min and 4 h post-infection with the aid of host RNA polymerase II (Theilmann and Stewart, 1992; Amer, 2011). In the present study, GFP expression preceded that of the RVFV S segment and the shRNA transcripts due to the very late baculovirus P_{PH} and P_{10} promoter activities. Transcripts of RVFV S-genome and GFP RNA were detected at as early as 24 h post-transfection, indicating that these very late P_{10} and immediate early *OpIE2* promoters respectively were already activated. These observations were in agreement with the documented data about properties of the baculovirus promoters. Once activated, the P_{PH} , P_{10} and *OpIE2* promoters remained activated throughout the course of this experiment and thus RNAi did not decrease the transcript levels to undetectable levels.

In conclusion, the BEVS experimental model shows that the high level RNA silencing against RVFV S-genome segment and GFP transcripts simultaneously is achievable using a single transgenic construct, and may provide new ideas and strategies of targeting the RVFV in the infected cells. Importantly, the model has demonstrated that the RVFV S-genome segment transcript is susceptible to RNA silencing. The findings suggest that by employing the use the multiple gene knockdowns in a single organism, the RNAi strategy could be applied to arrest or abrogate the *in vitro* and *in vivo* RVFV replications. By extension, the other two RVFV genome segments (L and M) can be silenced by the same multiplexed shRNA cassette designed in this study. Recent advances in RNAi applications make it possible to specifically suppress one or more genes simultaneously (Jung et al., 2017). Future studies should consider the next challenge of carrying out similar study using this or similar shRNA transcription cassette to target the wild type RVFV *in vitro* replication. Where, accordingly, in the design and the analyses, more appropriate internal controls, and more sensitive and

accurate transcript detection methods such as qPCR and western blots are incorporated in the analyses to confirm the effect and the degree of the *RNAi*. Broadly, the BEVS-based model is a suitable model for studying *RNAi* particularly for demonstrating simultaneous *RNAi* silencing of multiple sequences, in a multiplex *RNAi* using a single transgenic construct of defined size. Moreover, the model may be used in *RNAi* trials and testing the power of shRNA constructs by selecting and optimizing shRNA clones because the differential transcript levels and *siRNA* concentrations are quantifiable.

CONFLICT OF INTERESTS

The authors have not declared any conflict of interests.

ACKNOWLEDGEMENTS

This work was done as part of a larger on-going study in search for safe antiviral therapies that will offer effective treatment and prevention remedies to combat any future RVFV outbreaks. It was sponsored by Jomo Kenyatta University of Agriculture and Technology (JKUAT) research grant No. JKU/RPE/RPPC/RP/65 for the study entitled "Controlling Rift Valley Fever virus using RNA Silencing". The authors acknowledge the Center for Disease Control and Prevention (CDC), Nairobi, Kenya for supporting the virus isolation phase. Dr. M. Kariuki Njenga of CDC Kenya donated the RVFV isolate that was used in this work. They appreciate the technical support contributed by Leonard Nderitu and Solomon Gikundi in the CDC cell culture laboratory. They also acknowledge the support offered by the International Center of Insect Physiology and Ecology (*icipe*) Molecular Biology and Bioinformatics Unit (MBBU), Nairobi, Kenya for the molecular analyses phase. Particularly, they recognise Dr. Daniel Masiga for allowing this work to be done in his lab. They also appreciate Dr. Joel L. Bargul for offering technical assistance for the molecular and GFP fluorescence analyses.

REFERENCES

- Agrawal N, Dasaradhi PVN, Mohammed A, Malhotra P, Bhatnagar RK, Sunil KM (2003). RNA Interference: Biology, Mechanism, and Applications. *Microbiol. Mol. Biol. Rev.* 67:657-685.
- Amer HM (2011). Baculovirus expression vector system: An efficient tool for the production of heterologous recombinant proteins. *Afr. J. Biotechnol.* 10(32):5927-5933.
- Boshra H, Lorenzo G, Busquets N, Brun A (2011). Rift Valley Fever: Recent Insights into Pathogenesis and Prevention. *J. Virol.* 85(13):6098-6105.
- Braunagel SC, Summers MD (2007). Molecular biology of the baculovirus occlusion-derived virus envelope. *Curr. Drug Targets* 8(10):1084-1095.
- Breiman RF, Njenga MK, Cleaveland S, Sharif SK, Mbabu M, King L (2008). Lessons from the 2006–2007 Rift Valley fever outbreak in East Africa: Implications for prevention of emerging infectious diseases. *Future Virol.* 3:411-417.
- Brummelkamp TR, Bernards R, Agami R (2002). A system for stable expression of short interfering RNAs in mammalian cells. *Science* 296(5567):550-553.
- Bucher E, Lohuis D, van Poppel PMJA, Geerts-Dimitriadou C, Goldbach R, Prins M (2006). Multiple virus resistance at a high frequency using a single transgene construct. *J. Gen. Virol.* 87:3697-3701.
- Carmona S, Ely A, Crowther C, Moola N, Salazar FH, Marion PL (2006). Effective inhibition of HBV replication in vivo by anti-HBx short hairpin RNAs. *Mol. Ther.* 13(2):411-421.
- CDC-Centers for Disease Control and Prevention (2007). Rift Valley fever outbreak Kenya, November 2006-January 2007. *MMWR. Morbidity and mortality weekly report* 56:73-76.
- Chalfie M, Kain S (1998). Green fluorescent protein: properties, applications, and protocols. New York: Wiley-Liss.
- Chalfie M, Tu Y, Euskirchen G, Prasher DC (1994). Green fluorescent protein as a marker for gene expression. *Science* 263(5148):802-805.
- Chap TL (2003). *Introductory to Bioinformatics*. John Wiley and Sons Publishing Inc., Hoboken, New Jersey, pp. 209-313.
- Ciccarone VC, Polayes D, Luckow VA (1997). Generation of Recombinant Baculovirus DNA in *E. coli* Using Baculovirus Shuttle Vector. In *Methods Molec. Med.* Edited by U. Reisch. Humana Press Inc., Totowa, NJ. P 13.
- Collett MS, Purchio AF, Keegan K, Frazier S, Hays W, Anderson DK (1985). Complete nucleotide sequence of the M RNA segment of Rift Valley fever virus. *J. Virol.* 144:228-245.
- Collins TJ (2007). ImageJ for microscopy. *BioTechniques* 43(1):25-30.
- Daubney R, Hudson JR, Garnham PC (1931). Enzootic hepatitis or Rift Valley fever. An undescribed virus disease of sheep, cattle and man from East Africa. *J. Pathol. Bacteriol.* 34:545-579.
- Easterday BC, McGavran MH, Rooney JR, Murphy LC (1962). The pathogenesis of Rift Valley fever in lambs. *Am. J. Vet. Res.* 23:470-479.
- Elliott RM (1990). Molecular biology of the Bunyaviridae. *J. Gen. Virol.* 71:501-522.
- Ellis DS, Shirodaria PV, Fleming E, Simpson DI (1988). Morphology and development of Rift Valley fever virus in Vero cell cultures. *J. Med. Virol.* 24(2):161-174.
- Faburay B, Wilson WC, Gaudreault NN, Davis AS, Shivanna V, Bawa B, Sunwoo SY, Ma W, Drolet BS, Morozov I, McVey DS (2016). A Recombinant Rift Valley Fever Virus Glycoprotein Subunit Vaccine Confers Full Protection against Rift Valley Fever Challenge in Sheep. *Sci. Rep.* 6:27719.
- Fisher LD, Belle GV (2004). *Biostatistics: A methodology for the health sciences*. Heagerty P. J and Lumley T. 2nd edition. John Wiley and Sons Inc., Hoboken, New Jersey, pp. 123-133.
- Fitzgerald K, White S, Borodovskiy A, Bettencourt BR, Strahs A, Clausen V, Wijngaard P, Horton JD, Taubel J, Brooks A, Fernando C (2017). A Highly Durable RNAi Therapeutic Inhibitor of PCSK9. *New Engl. J. Med.* 376:41-51.
- Ge Q, Eisen HN, Chen J (2004). Use of siRNAs to prevent and treat influenza virus infection. *J. Virus Res.* 102(1):37-42.
- Giorgi C, Accardi L, Nicoletti L, Gro MC, Takehara K, Hilditch C, Morikawa S, Bishop DH (1991). Sequences and coding strategies of the S RNAs of Toscana and Rift Valley fever viruses compared to those of Punta Toro, Sicilian Sandfly fever, and Uukuniemi viruses. *J. Virol.* 180:738-753.
- Giorgi C (1996). Molecular biology of phlebovirus. In: *The Bunyaviridae*, Edited by R. M. Elliott. New York: Plenum Press. Pp. 105-128.
- Hannon GJ (2002). RNA interference. *Nature* 418:244-251.
- Hannon GJ, Rossi JJ (2004). Insightful review articles: Unlocking the potential of the human genome with RNA interference. *Nature* 431:371-378.
- Harris R, Polayes D (1997). A New Baculovirus Expression Vector for the Simultaneous Expression of Two Heterologous Proteins in the Same Insect Cell. *Focus* 19:6-8.
- Ikegami T, Makino S (2009). Rift Valley fever vaccines. *Vaccine* 27(S4):D69-D72.
- Jung J, Nayak A, Schaeffer V, Starzetz T, Kirsch AK, Müller S, Dikic I, Mittelbronn M, Behrends C (2017). Multiplex image-based autophagy RNAi screening identifies SMCR8 as ULK1 kinase activity and gene expression regulator. *eLife* 6:e23063.

- Kang S, Hong YS (2008). RNA Interference in Infectious Tropical Diseases. *Korean J. Parasitol.* 46(1):1-15.
- Kaps M, Lamberson WR (2004). *Biostatistics for Animal Science*. CAB international publishing, UK, pp. 53-153.
- Koch A, Biedenkopf D, Furch A, Weber L, Rossbach O, Abdellatef E, Linicus L, Johannsmeier J, Jelonek L, Goesmann A, Cardoza V (2016). An RNAi- Based Control of *Fusarium graminearum* Infections Through Spraying of Long dsRNAs Involves a Plant Passage and Is Controlled by the Fungal Silencing Machinery. *PLoS Pathog.* 12(10):e1005901.
- Li S, Patel DJ (2016). Droscha and Dicer: Slicers cut from the same cloth. *Cell Res.* 26:511-512.
- Linthicum KJ, Anyamba A, Tucker CJ, Kelley PW, Myers MF, Peters CJ (1999). Climate and satellite indicators to forecast Rift Valley fever epidemics in Kenya. *Science* 285:397-400.
- Liu DY, Tesh RB, Travassos D, Rosa AP, Peters CJ, Yang Z, Guzman H, Xiao SY (2003). Phylogenetic relationships among members of the genus *Phlebovirus* (Bunyaviridae) based on partial M segment sequence analyses. *J. Gen. Virol.* 84:465-473.
- McCaffrey AP, Meuse L, Pham TT, Conklin DS, Hannon GJ, Kay MA (2002). Gene expression: RNA interference in adult mice. *Nature* 418:338-339.
- McGinnis KM (2010). RNAi for functional genomics in plants. *Brief. Funct. Genomics* 9(2):111-117.
- Meegan JM, Hoogstraal H, Moussa MI (1979). An epizootic of Rift Valley fever in Egypt in 1977. *J. Vet. Res.* 105:124-125.
- Meegan JM, Watten RH, Laughlin LW (1981). Clinical experience with Rift Valley fever in humans during the 1977 Egyptian epizootic. *Contribution on Epi Biostat* 3:114-123.
- Meng Z, Zhang X, Wu J, Pei R, Xu Y, Yang D, Roggendorf M, Lu M (2013). RNAi Induces Innate Immunity through Multiple Cellular Signaling Pathways. *PLoS One* 8(5):e64708.
- Muller R, Poch O, Delarue M, Bishop DHL, Bouloy M (1994). Rift Valley fever virus L segment: correction of the sequence and possible functional role of newly identified regions conserved in RNA-dependent polymerases. *J. Gen. Virol.* 75(6):1345-1352.
- Nderitu L, Lee JS, Omolo J, Omulo S, O'Guinn ML, Hightower A, Mosha F, Mohamed M, Munyua P, Nganga Z, Hiett K, Seal B, Feikin DR, Breiman RF, Kariuki MN (2011). Sequential Rift Valley Fever Outbreaks in Eastern Africa Caused by Multiple Lineages of the Virus. *J. Infect. Dis.* 203(5):655-665.
- Nichol ST, Beaty BJ, Elliott RM, Goldbach RW, Plyusnin A, Tesh RB (2005). Classification and nomenclature of viruses. VIIIth report of the International Committee on Taxonomy of Viruses. In: *The Bunyaviridae, Virus taxonomy*. Edited by C. Fauquet, M.A. Mayo, L.S.M. Maniloff, U. Desselberger & L.A. Ball. Elsevier Academic Press, London. pp. 695-716.
- Nishitsuji H, Kohara M, Kannagi M, Masuda T (2006). Effective suppression of human immunodeficiency virus type 1 through a combination of short- or long-hairpin RNAs targeting essential sequences for retroviral integration. *J. Virol.* 80(15):7658-7666.
- O'Reilly DR, Miller LK, Luckow VA (1992). *Baculovirus Expression Vectors: A Laboratory Manual*, W. H. Freeman and Company, New York.
- Pepin M, Bouloy M, Bird BH, Kemp A, Paweska J (2010). Rift Valley fever virus (*Bunyaviridae: Phlebovirus*): an update on pathogenesis, molecular epidemiology, vectors, diagnostics and prevention. *J. Vet. Res.* 41(6):61.
- Pompey JM, Morf L, Singh U (2014). RNAi Pathway Genes Are Resistant to Small RNA Mediated Gene Silencing in the Protozoan Parasite *Entamoeba histolytica*. *PLoS One* 9(9):e106477.
- Sang R, Arum S, Chepkorir E, Mosomtai G, Tigoi C, Sigei F, Lwande OW, Landmann T, Affognon H, Ahlm C, Evander M (2017). Distribution and abundance of key vectors of Rift Valley fever and other arboviruses in two ecologically distinct counties in Kenya. *PLoS Negl. Trop. Dis.* 11(2):e0005341.
- Shi JY, Liu B, Wang M, Luo EJ (2010). Short hairpin RNA-mediated inhibition of measles virus replication *in vitro*. *Can. J. Microbiol.* 56:77-80.
- Sindato C, Pfeiffer DU, Karimuribo ED, Mboera LEG, Rweyemamu MM, Paweska JT (2015). A Spatial Analysis of Rift Valley Fever Virus Seropositivity in Domestic Ruminants in Tanzania. *PLoS One* 10(7):e0131873.
- Swamy MN, Wu H, Shankar P (2016). Recent advances in RNAi-based strategies for therapy and prevention of HIV-1/AIDS. *Adv. Drug Deliv. Rev.* 103:174-86.
- Swanepoel R, Coetzer JAW (2004). Rift Valley fever, In: *Infectious diseases of livestock*, Edited by J. A. W. Coetzer & R. C. Tustin. Oxford University Press, Cape Town, South Africa. Pp. 1037-1070.
- Tamura K, Dudley J, Nei M, Kumar S (2007). MEGA4: Molecular Evolutionary Genetics Analysis (MEGA) software version 4.0. *Mol. Biol. Evol.* 24:1596-1599.
- Theilmann DA, Stewart S (1992). Molecular Analysis of the trans-Activating IE-2 Gene of *Orgyia pseudotsugata* Multicapsid Nuclear Polyhedrosis Virus. *J. Virol.* 187:84-96.
- Vlak JM, Keus RJA (1990). Baculovirus Expression Vector System for Production of Viral Vaccines. In: *Viral Vaccines*, Wiley-Liss Inc. pp. 91-128.
- WHO-World Health Organization (2007). Rift Valley Fever outbreak-Kenya, November 2006-January 2007. *MMWR. Morbidity and Mortality Weekly Report* 56:73-76.
- Yang S, Miller LK (1999). Activation of Baculovirus Very Late Promoters by Interaction with Very Late Factor 1. *J. Virol.* 73(4):3404-3409.

SUPPLEMENTARY INFORMATION

Table S1. Average concentrations of the total RNA of duplicate *in vitro* transcription time-course experiments.

Time (h)	Total RNA ($\mu\text{g/mL}$)		
	Un-transfected control cells	<i>siRNA-negative</i>	<i>siRNA-positive</i>
0	863.10	325.45	700.40
24	429.64	661.88	611.06
48	515.76	652.86	644.94
72	406.18	489.84	556.08
96	578.26	1312.14	707.54

Table S2. Computation of relative GFP fluorescence using the Image J 1.45 software.

Big boxes (Within the cells)	Area	Mean	Raw integrated density
1	22528	27.89	628295
Small boxes (Background outside the cells)	Area	Mean	Raw integrated density
2	420	6	2520
3	210	6	1260
4	196	5.98	1172
5	208	6.096	1268
		Mean of means	Corrected integrated density
Mean of Means		6.019	
Corrected integrated density			492698.968

The ImageJ software was used to automatically measure the parameters highlighted in red in the excel image example below. The regions within the images of *Sf21* cells emitting the GFP fluorescence were selected. The same readings were scored for the background smaller selections outside the fluorescing cells. All the readings were exported to spread sheet where the averages were computed. The cells incubated at different time points (0, 24, 48, 72 and 96 h) from the time-course experiments were analyzed separately. The averages from the two independent experiments were summarized in Table 4. To compute the corrected integrated density (Relative GFP fluorescence) the following formular was used; Corrected Integrated Density (relative GFP fluorescence) = (The difference between the Average raw intensity readings within the *Sf21* cells and the means of means of the background readings outside the cells) multiplied by the average area selected within the *Sf21* cells.

Table S3. Time-course correlation of relative GFP fluorescence, set 1.

x_i	y_i	$x_i - \bar{x}$	$(x_i - \bar{x})^2$	$y_i - \bar{y}$	$(y_i - \bar{y})^2$	$Dx Dy$
0	0	-48	2304	-2.86	8.17	137.21
24	1.40046018	-24	576	-1.46	2.13	34.99
48	2.08556495	0	0	-0.77	0.60	0.0
72	3.69000036	24	576	0.83	0.69	19.96
96	7.11857	48	2304	4.26	18.13	204.39
Sum			5760		29.72	396.55

$r = 0.9584$; $r^2 = 0.9186$

Table S4. Time-course correlation of relative GFP fluorescence, set 2.

x_i	y_{ii}	$x_i - \bar{x}$	$(x_i - \bar{x})^2$	$y_{ii} - \bar{y}$	$(y_{ii} - \bar{y})^2$	$DxDy$
0	0	-48	2304	2.69	7.21	128.90
24	0.50607173	-24	576	-2.18	4.75	52.30
48	2.3809691	0	0	-0.30	0.09	0
72	3.3460522	24	576	0.66	0.44	15.86
96	7.1935507	48	2304	4.51	20.32	216.39
Sum			5760		32.81	413.45

$r = 0.9511$; $r^2 = 0.9045$.

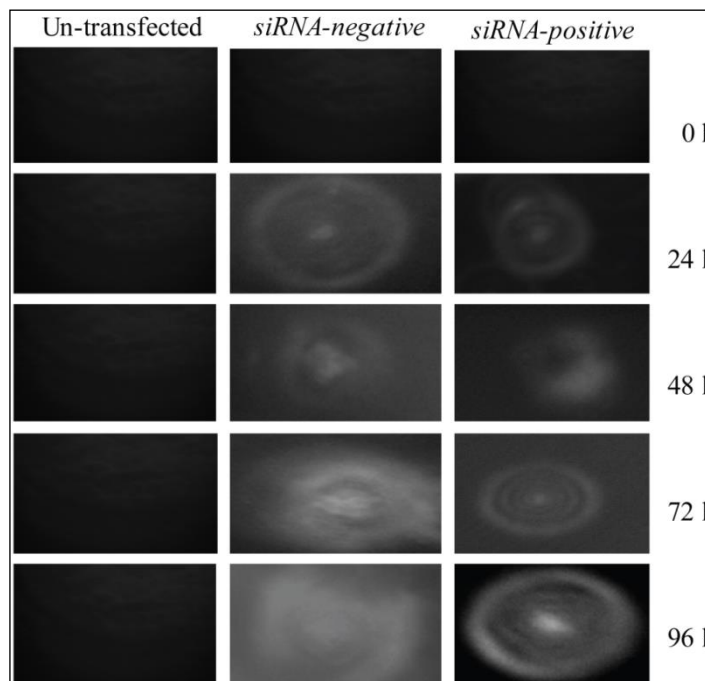


Figure S1. The relative GFP fluorescence per cell. Column 1: Un-transfected Sf21 cell (Control group). Column 2: GFP fluorescence in the Sf21 test cell (RNAi-negative group). Column 3: Declined GFP fluorescent intensity in Sf21 cell (RNAi-positive group).

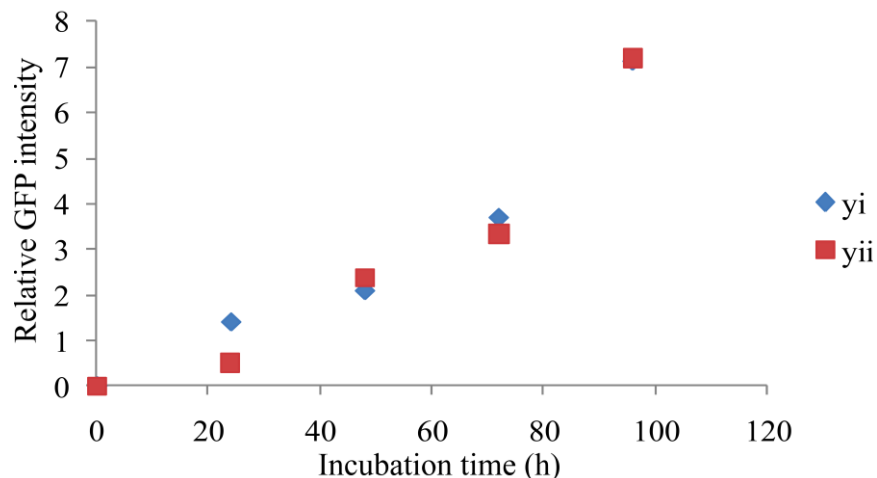


Figure S2. Apparent positive correlation between x and y .

Here below, t statistic analyses are provided in detail.

To answer the question whether there was linear association between the incubation time and amount of change in the relative GFP fluorescence, the sums of squares and sum of products were computed as follows: $SS_{xx} = 5760$, $SS_{yy} = 29.72$ and $SS_{xy} = 396.55$ in set 1 and $SS_{xx} = 5760$, $SS_{yy} = 32.81$ and $SS_{xy} = 413.45$ in set 2. The average sums of squares and sum of products from both sets were $SS_{xx} = 5760$, $SS_{yy} = 31.05$ and $SS_{xy} = 404.5$.

Using the average sums of squares and sum of products, the sample coefficient of correlation was:

$$r = \frac{SS_{xy}}{\sqrt{SS_{xx} SS_{yy}}} = \frac{404.5}{\sqrt{(5760)(31.05)}} = 0.96$$

The calculated value of the t statistic was:

$$t = \frac{r\sqrt{n-2}}{\sqrt{1-r^2}} = \frac{0.96\sqrt{5-2}}{\sqrt{1-0.96^2}} = 17.3$$

The critical value with 5% significance level and 3 degrees of freedom (df) was:

$$t_{\alpha/2,3} = t_{0.25/3} = 3.18$$

The calculated $t = 17.3$ was more extreme than 3.18, so H_0 is rejected. There is linear association between incubation time and amount of change in relative GFP fluorescence due to *RNAi*.

Hypothesis of no difference ($H_0: \mu = 0$) that the *RNAi*-positive had no effect based on the relative GFP fluorescence between *RNAi*-negative and *RNAi*-positive groups in the two sets was tested. Considering the values from 24 h incubation, df was $4-1 = 3$.

The t -statistic for the set 1 was:

$$t = \frac{\bar{x}_d - c}{S_d / \sqrt{n}} = \frac{357315.28 - 0}{254970.85 / \sqrt{4}} = 2.80$$

The t -statistic in set 2 was:

$$t = \frac{\bar{x}_d - c}{S_d / \sqrt{n}} = \frac{335666.09 - 0}{281659.79 / \sqrt{4}} = 2.38$$

The critical t -statistic value for 3 df at 95% ($\alpha = 0.05$) confidence level $t_{1-0.05/1,3} = 2.3534$ hence P value for these statistics was <0.05 . This indicated that the observed values clearly fell into the rejection regions, hence the null hypothesis were rejected.

Differences in the amount of change were also tested by comparing their means between the two sets. The null hypothesis was that the mean change between set 1 and set 2 groups was equal ($H_0: \mu_1 = \mu_2$). Both sample standard deviations were used to compute the "pooled" standard deviation which has n_1+n_2-2 df . Brown-Forsythe (BF) test, which is a 2-sample t -test that looks at the spread of the data in absolute terms, was used. The BF test is usually used with comparison of multiple groups in analyses of variance but may be used with 2 groups. To compute the BF statistic, first the median of each group was calculated, mdi , and then computed the absolute value of the difference between each sample and its group median.

$$S_p = \sqrt{\frac{(n_1 - 1)S_1^2 + (n_2 - 1)S_2^2}{n_1 + n_2 - 2}} = \sqrt{\frac{(4 - 1)281659.79^2 + (4 - 1)281659.79^2}{4 + 4 - 2}} = 268646.95$$

The t -statistic for these data with 6 df considering values from 24 h incubation was:

$$t = \frac{357315.28 - 335666.09}{(268646.95)\sqrt{\frac{1}{4} + \frac{1}{4}}} = 0.0806$$

The critical t value for 6 (n_1+n_2-2) df at 95% ($\alpha = 0.05$) confidence level, $t_{1-0.05/1,6} = 1.9432$ hence P value for this statistic is >0.05 . This observed values clearly fell into the acceptance region in favour of null hypothesis. Hence the null hypothesis was accepted and concluded that the average in relative GFP fluorescence observed in set 1 was not significantly different from that observed in set 2 in terms of the amount of change.

```

>GGATCCAGAGAACCTTTGATAAATCATAGTCTTTGCTGGAGCACCGACCTGTTTC
TAGAACTTTCCTAACTGAGGCTCTCCCCATCTTAGAAATAGCATAATCAACAAACTT
ATCCATCAAGGGATGAGCAATCATAGATAATGAACTGATGTCTACTAGTCACATTT
TAGAGAGGCCTGTTCTTCCAAGATATATAAGGAGGAAGAAGAGCCCAATTGATAAT
GCAACATACAGGCAAATGAGGAGTATAGTTTTAAGCGGCCCTCCAAACCAACTCAT
GAGTCCAGAAAACCAGTCAAAGAAATTCCAAGCGGCCGCCTTCCTGTCACTGGGA
CAACCATGGACGGTCTATCCCCTGCGTACCCGAGGCATATGATGCATCCCAGCTTT
GCTGGCATGGTGGACCCCTTCTACCAGAAGACTATCTAAGGGCAATATTAGATGC
TCACTCTGTGTATCTGCTGCAGTTCTCTTATGGTGTTCATGCTTTTCCCGTTATCC
GGATCATATGAAACGGCATGACTTTTTCAAGAGTGCCATGCCCGAAGGTTATGTAC
AGGAACGCACTATATCTTTCAAAGATGACGGGAACTACAAGACGCGTGCTGAAGTC
AAGTTCAAGAGAATTCCTTGACTTCAGCACGCGTCTTGTAGTTCCCGTCATCTTTG
AAAGATATAGTGCCTTCTGTACATAACCTTCGGGCATGGCACTCTTGAAAAAGTC
ATGCCGTTTCATATGATCCGGATAACGGGAAAAGCATTGAACACCATAAGAGAACT
GCAGCAGATACAGAGAGTGAGCATCTAATATTGCCCTTAGATAGTCTTCTGGTAGA
GAAGGGTCCACCATGCCAGCAAAGCTGGGATGCATCATATGCCTCGGGTACGCAG
GGGATAGACCGTCCATGGTTGTCCCAGTGACAGGAAGGCGGCCGCTTGGAATTTCC
TTTGACTGGTTTTCTGGACTCATGAGTTGGTTTTGGAGGGCCGCTTAAACTATACT
CCTCATTGCTGTATGTTGCATTATCAATTGGGCTCTTCTTCTCCTTATATATCTT
GGAAGAACAGGCCTCTCTAAAATGTGACTAGTAGGACATCAGTTCATTATCTATGA
TTGCTCATCCCTTGATGGATAAGTTTGTGGATTATGCTATTTCTAAGATGGGGAGAG
CCTCAGTTAGGAAAGTTCTAGAAACAGGTCCGGTGCTCCAGCAAAGACTATGATTTA
TCAAAGGTTCTCTAAGCTT

```

Figure S3. Complete 1253 bp shRNA transcription cassette as was confirmed by Sanger sequencing. Total RNA was isolated from each of the Sf21 cells that were un-transfected or co-transfected with pIZ/V5-GFP and either the recombinant AcMNPV Bacmid-S or AcMNPV Bacmid-S/shRNA was harvested at 0, 24, 48, 72 and 96 h post-transfection. The total RNA samples isolated from control cells was also quantified (Materials and Methods) and recorded. The average concentrations of the total RNA isolated from the duplicate *in vitro* transcription time-course experiments were determined (Table S1). ***The bases highlighted in colour were gene specific sequences used to construct the multiplex shRNA transcription cassette. The colour code representation is as follows:

1. **Yellow:** shRNA sequences from RVFV L genome segment.
2. **Pink:** shRNA sequences from RVFV M genome segment.
3. **Turquoise:** shRNA sequences from RVFV S-genome segment.
4. **Bright green:** shRNA sequences from GFP.
5. **Grey:** A 13 bp loop (Spacer) separating the genomic sense and reverse complement shRNA constructs.
6. **Italicized bases:** Restriction enzyme sites used in the construction of the shRNA transcription cassette.